Journal of Building Engineering 121 (2026) 115755

Contents lists available at ScienceDirect

Journal of Building Engineering

journal homepage: www.elsevier.com/locate/jobe

Full length article

Sand-free olive kernel aggregate mortars for sustainable building applications: Mechanical and hygrothermal characterization

Nicolò Lo Presti [a,*], Kamilia Abahri [b], Mohamed Soufiane Ghomchi [b], Paolo Stabellini [c], Giovanni Castellazzi [a]

[a] Department of Civil, Chemical, Environmental and Materials Engineering (DICAM), University of Bologna, Viale del Risorgimento 2, Bologna, 40136, Italy
[b] Université Paris-Saclay, ENS Paris-Saclay, CentraleSupélec, CNRS, LMPS - Laboratoire de Mécanique Paris-Saclay, Gif-sur-Yvette, 91190, France
[c] EDILTECO S.p.A., Via dell'Industria 710, San Felice sul Panaro, 41038, Italy

ARTICLE INFO

Keywords:
Bio-based building materials
Agricultural waste valorization
Sustainable composites

ABSTRACT

This study explores the valorization of Olive Kernel Aggregate (OKA) as a total substitute for mineral sand in cementitious mortars, addressing the critical need for bio-based alternatives in the construction sector. While previous research on sand-free OKA mortars relied on high cement dosages ($> 600\,kg/m^3$) to ensure mechanical resistance, this approach often compromises the overall sustainability of the composite. To overcome this limitation, this work investigates the mechanical and hygrothermal performance of mortars produced with moderate binder contents ($300 - 500\,kg/m^3$). The experimental campaign coupled standard mechanical testing and microstructural analysis (SEM, XRD) with an in-depth hygric characterization, including Water Vapor Permeability and Moisture Buffer Value (MBV) assessments. The results reveal that reducing the cement dosage significantly enhances the insulating properties and moisture buffering capacity, achieving an "Excellent" MBV classification according to the NORDTEST protocol. Conversely, increasing the binder content to $400\,kg/m^3$ yields a compressive strength of approximately 13 MPa, demonstrating that structural adequacy for specific building applications can be attained with significantly lower clinker content than current literature benchmarks. The discussion highlights a clear trade-off between mechanical strength and hygrothermal comfort, suggesting that these sand-free composites are viable for sustainable building applications ranging from lightweight insulating fillers to moderate load-bearing floor screeds.

1. Introduction

The built environment is estimated to be responsible for 37% of global carbon emissions [1]. In 2021, emissions associated with the construction and demolition of a building accounted for one-third of the operational emissions, which are generated during the building's use and maintenance. Operational emissions are expected to decrease as electricity grids transition to renewable energy; consequently, embodied emissions could account for roughly 50% of total building emissions by 2050 if no action is taken [1]. Cement and aggregates, the main constituents of concrete, are the most used materials in buildings. Global cement manufacturing is responsible for 7% of carbon emissions, while sand and gravel are the most consumed raw materials on earth after water, with an extraction rate that far exceeds natural renewal [2,3].

* Corresponding author.
E-mail address: nicolo.lopresti2@unibo.it (N. Lo Presti).

https://doi.org/10.1016/j.jobe.2026.115755
Received 1 October 2025; Received in revised form 16 February 2026; Accepted 27 February 2026
Available online 28 February 2026

Currently, researchers are exploring approaches to reduce the environmental impact of concrete and cement-based materials, e.g., lowering the carbon emissions of cement plants [4], using supplementary cementitious materials as partial replacement for clinker [5–7] or through the use of recycled concrete aggregates in concrete mixtures [8,9]. When moderate structural performances are needed, biomass waste can be used as a partial or total substitute of aggregates to produce lightweight materials with low or negative carbon footprint. These reduce the operational emissions of buildings thanks to their enhanced insulating performances and keep carbon out of the atmosphere, supporting the strategy of using buildings as a global carbon sink [10,11]. Several efforts are being made to replace traditional aggregates in mortars with various types of biomass, such as wood shavings, straw, cork, rice husk, coconut shell, flax or hemp shives [12–14], e.g., focusing on their influence on the insulating performance [15], the optimization of mix design for 3D printing applications [16], the influence of aging on hygrothermal and mechanical properties [17] and the recycling potential after deconstruction [18].

Another biomass abundantly available in countries of the Mediterranean area is the crushed olive kernel, a by-product of the olive oil industry. While few research contributions are available in the literature concerning its valorization in the building construction sector, interest is growing. Researchers are exploring its potential by investigating its viability in the calcined form as a replacement for clinker in cements [19], the production of polyester resin-bound particle boards [20] and the manufacturing of sustainable mortar bricks for facades [21,22].

Recent studies have also explored the use of olive oil waste ash (OA) as a cementitious addition. For instance, Al-kheetan et al. [23] used OA as a partial cement replacement (up to 15%) in pavement concrete, optimizing it with nano-silica to improve mechanical and durability performance. Similarly, Safouene et al. [24] investigated the incorporation of olive waste ash (3%–12%) in rigid pavement concrete, noting a slight decrease in compressive strength but an improvement in tensile performance. Regarding the environmental impact, Mohamed et al. [25] provided a review of biomass ashes derived from olive stones, summarizing their effects on mechanical properties and potential economic benefits. El-Hassan et al. [26] and Los Añez et al. [27] further addressed the sustainable valorization of olive by-products through life cycle assessments (LCA), highlighting the environmental benefits of using ground olive stones as partial aggregate replacements under specific mix design and transport conditions. Martin et al. [28] and Del Rio Merino et al. [29] examined the viability of lightweight mortars using whole, crushed, or calcined olive stones as partial replacements for traditional aggregates, confirming technical feasibility with adjustments in setting times.

The potential of employing crushed Olive Kernel Aggregate (OKA) specifically as a substitute for traditional mineral sand in mortars has been examined in specific investigations. Barreca and Fichera [30] replaced up to 70% of sand with OKA in cement-lime mortars, focusing on hygrothermal properties. They achieved a thermal conductivity of 0.266 W/(mK) at a density of 1148 kg/m^3, demonstrating the potential for insulating building components such as lightweight screeds and plasters. Ferreiro-Cabello et al. [31] investigated the mechanical performance of OKA-based mortars with different cement types. They reported difficulties in handling and insufficient strength at replacement levels above 50%. Their results showed that mortars with 30% OKA substitution using CEM I 52.5 R achieved a compressive strength of approximately 12 MPa and a flexural strength of 1.4 MPa at 28 days. Boukhelkhal et al. [32] developed self-compacting mortars with OKA substitution up to 50%, using 678 kg/m^3 of CEM II/A 42.5 cement. At this replacement level, they obtained a density of 1500 kg/m^3, a compressive strength of 15 MPa, and a thermal conductivity of 0.689 W/(mK). Cheboub et al. [33] is the only study that achieved complete (100%) substitution of sand with OKA in self-compacting lightweight mortars. From their reported data, it can be estimated that they used a cement dosage exceeding 650 kg/m^3 of CEM II/B 42.5 N. Their 100% OKA formulation achieved a hardened density of 1410 kg/m^3, a compressive strength of approximately 7 MPa at 28 days (increasing to 15 MPa at 91 days), and a thermal conductivity of about 0.35 W/(mK). These results suggest the potential for manufacturing lightweight insulating screeds, though the high cement dosage may limit the overall sustainability of the approach.

Maximizing the carbon storage potential of bio-based mortars requires increasing the incorporated biomass while simultaneously limiting the cement content, which represents the main source of CO_2 emissions. However, the literature review reveals that only Cheboub et al. [33] explored the total substitution of traditional sand with OKA. Nevertheless, the high cement dosage employed in that study, around 650 kg/m^3, although likely enhancing mechanical performance, might limit the overall sustainability of the material. Consequently, the challenge lies in enhancing mechanical and hygrothermal properties through optimized formulations capable of balancing structural performance and environmental impact.

Addressing this gap, this paper presents the results of an experimental campaign conducted on 100% OKA-based mortars produced with moderate binder dosages. The primary objective is to extend the findings of previous research by validating the feasibility of lower cement dosages, a significant challenge given the potential decrease in mechanical properties and workability associated with full sand replacement. Furthermore, this study provides a comprehensive characterization of both mechanical and hygrothermal properties. Beyond standard mechanical strength, thermal insulation, and porosity, this work assesses water vapor permeability and the Moisture Buffer Value (MBV), properties that, to the best of our knowledge, have never been evaluated for OKA-based mortars. This holistic dataset is intended to support informed applications in sustainable building practices. Portland cement was selected as the binder to facilitate comparison with existing literature and ensure immediate applicability in the construction industry without requiring specialized workforce training, although future research may explore alternative low-carbon binders.

Section 2 describes the adopted materials and methods. The results obtained during the experimental characterization campaign are presented in Section 3, while a critical discussion is provided in Section 4. Concluding remarks are given in Section 5.

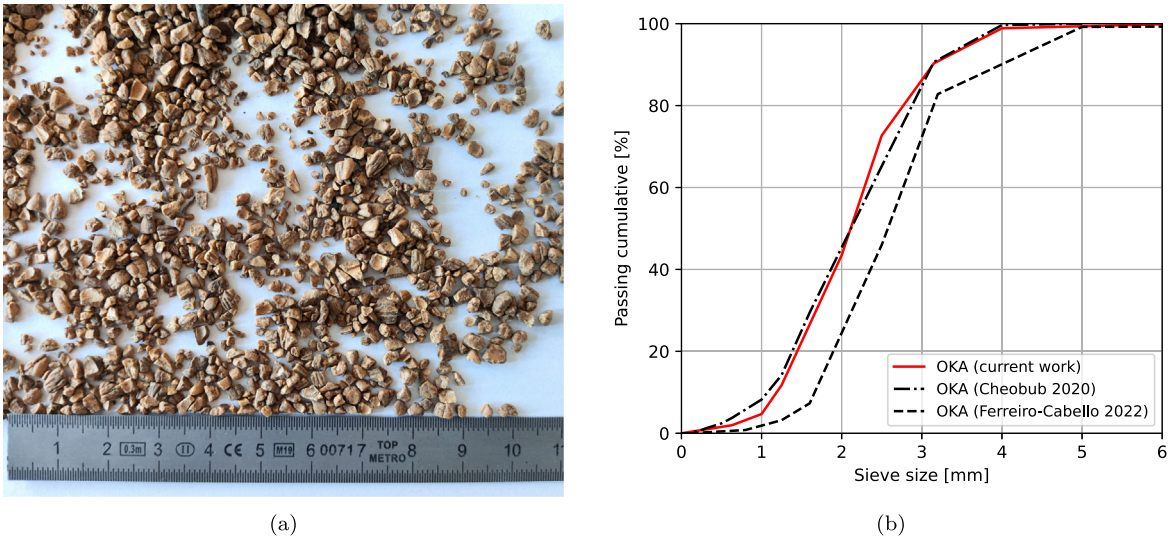

Fig. 1. Magnification of particles (a) and granulometric curve (b) of the olive kernel aggregate employed in this research. *Source:* Adapted from [34].

Table 1
Properties of the OKA adopted in this work, adapted from [34].

Property	Unit	Raw OKA	Fine OKA
w_0	[kg/kg]	0.129	0.129
ρ_b	[kg/m^3]	755	730
ρ_{ssd}	[kg/m^3]	1365	1365
ρ_{rd}	[kg/m^3]	1079	1073
ρ_a	[kg/m^3]	1512	1516
w_{24}	[kg/kg]	0.265	0.272

2. Materials and methods

2.1. Materials

2.1.1. Olive kernel aggregate

The Olive Kernel Aggregate (OKA) used in this work, previously employed and characterized in [34], is a waste product derived from the production process of olive oil. The pomace exiting the olive mill is processed to remove oil residues and fine particles to obtain the OKA depicted in Fig. 1(a). For completeness, its characterization is briefly summarized below. As shown in Fig. 1(b), particle size mainly ranges between 0.5 mm and 4 mm. Moreover, the same figure shows a granulometric distribution similar to that of OKA used by Cheboub et al. [33] and Ferreiro-Cabello et al. [31].

To investigate the influence of the particle size of the aggregate, two variants of the OKA were used. The first, referred to as raw OKA, is the aggregate as provided by the supplier; the second, termed fine OKA, is a finer version of the raw OKA obtained by removing larger particles that did not pass through a 2.5 mm sieve. The characterization of the OKA was carried out separately for its two versions to highlight potential differences due to the granulometry, and the results are shown in Table 1. In detail, the initial moisture content w_0 was determined on the basis of mass measurements of three samples, stabilized at a temperature of 23 °C and a relative humidity (RH) of 50%, and after being dried in an oven at 110 °C for 72 h. The loose bulk density ρ_b was measured on samples preconditioned at 23 °C and 50% RH according to ISO 20290-1:2021 [35]. Following UNI EN 1097-6:2022 [36], the pycnometer method was used to derive the saturated surface-dried particle density ρ_{ssd}, oven-dried particle density ρ_{rd}, apparent particle density ρ_a and water absorption after immersion for 24 h, w_{24}.

Measurements carried out on the raw and fine OKA demonstrate that the two aggregates overall possess very similar properties. As shown in Table 1, differences greater than 1% were observed only for w_{24}, which was 2.6% higher for fine OKA than for raw OKA, likely due to its higher specific surface area, and for ρ_b, which was 3.3% lower for fine OKA because of its different granulometric distribution.

In addition to the characterization reported in our previous study [34], the present work includes an assessment of the hygroscopic behavior of the aggregate. The water vapor sorption and desorption behavior were measured on three different representative samples by means of the Dynamic Vapor Sorption (DVS) Intrinsic PLUS device shown in Fig. 2(a). A single test

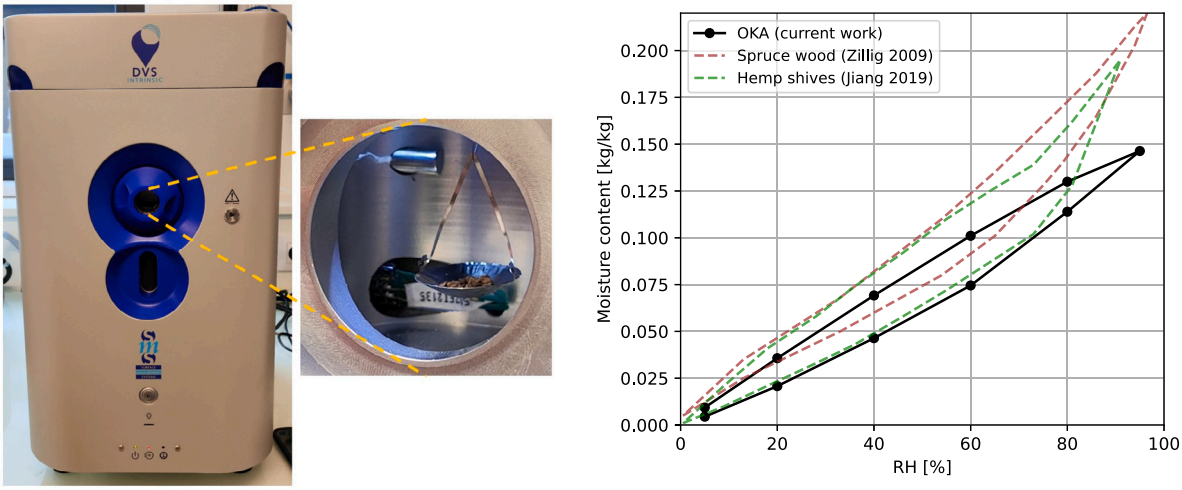

(a) (b)

Fig. 2. OKA sample positioned within the DVS apparatus (a), water vapor sorption-desorption isotherm of OKA compared with literature data for spruce wood [38] and hemp shives [37] (b).

lasted roughly 40 days and consisted of increasing relative humidity levels (5%, 20%, 40%, 60%, 80%, and 95%) to obtain the sorption branch of the isotherm, followed by decreasing them to derive the desorption branch, all at a constant temperature of 20 °C.

The resulting isotherms, illustrated in Fig. 2(b), compare the experimental data for OKA with literature values for hemp shives [37] and spruce wood [38]. The sorption branch of OKA closely follows that of hemp shives up to 80% RH; beyond this threshold, OKA reaches a moisture content of approximately 0.15 kg/kg at 90% RH, while hemp shives attain 0.18 kg/kg. Similarly, the spruce wood trend remains parallel to OKA up to 60% RH before diverging significantly to a value of 0.22 kg/kg at 90% RH. Consistent with the reference materials, OKA exhibits pronounced hysteresis. These differences are likely attributable to the more compact structure of OKA, which limits its capacity for moisture uptake compared to more porous bio-based materials. Nevertheless, despite the lower equilibrium moisture content at high RH, the hygric profile of OKA remains fundamentally comparable to those of wood and hemp.

2.1.2. Cement and superplasticizer

The cement used was a Portland CEM I 52.5N. Mortars were then obtained by mixing the solid constituents with tap water and the admixture CHRYSO Premia 570, a polycarboxylate-based superplasticizer with a suggested dosage between 0.8% and 3% of cement weight.

2.2. Methods

2.2.1. Samples preparation

Five different mortar formulations were studied in this work, expanding upon the three formulations investigated in our previous study [34]. Three of them consisted of a fixed mass of raw OKA, equal to 800 g, and a varying dosage of cement, specifically 300 g, 400 g and 500 g. An initial attempt to maintain the same Water/Cement (W/C) ratio resulted in the inability to achieve the same consistency for all mortars, even with considerable adjustments of the dosage of superplasticizer. Nevertheless, as the challenge here is to obtain performing composites produced with low cement dosages, it was decided to set the amount of superplasticizer equal to 2% by mass of cement, a dosage within the limits suggested by the manufacturer, and to adjust the water content to maintain the same consistency for the three mortars produced, namely F300A, F400A and F500A. The two other formulations, F300B and F400B, conceived to study the influence of the granulometric distribution, were obtained considering a fixed mass of fine OKA, equal to 800 g, a binder dosage of 300 g and 400 g, an amount of superplasticizer equal to 2% by mass of cement and the same W/C ratio adopted for mortars F400A and F300A. The list of formulations and the adopted quantities of constituents are reported in Table 2.

Fresh mortars were obtained by mixing all constituents in a mechanical mixer compliant with standard UNI EN 196-1:2016 [39]. Immediately after mixing, fresh mortars were poured into a container of known volume and weighed to determine the fresh density. For each formulation, three prismatic specimens of 4 cm × 4 cm × 16 cm, meant to be used for the mechanical characterization, were prepared by pouring the fresh mortar in molds following the procedure specified in UNI EN 1015-11:2019 [40]. Moreover, four cylindrical samples with a diameter of 11.3 cm and a height of 5 cm, for a total volume of 500 cm^3, were produced to be used for the characterization of moisture-related properties of hardened mortars. Immediately after the completion of the pouring phase, molds were covered with a plastic film and stored at 22 °C for 7 days. After this initial period, the samples were demolded and

Table 2
Mortar formulations.

Formulation	Raw OKA [g]	Fine OKA [g]	Cement [g]	Plastic. [g]	W/C [–]	Fresh dens. [kg/m^3]
F500A	800	–	500	10	0.42	1406
F400A	800	–	400	8	0.46	1286
F300A	800	–	300	6	0.56	1190
F400B	–	800	400	8	0.46	1277
F300B	–	800	300	6	0.56	1151

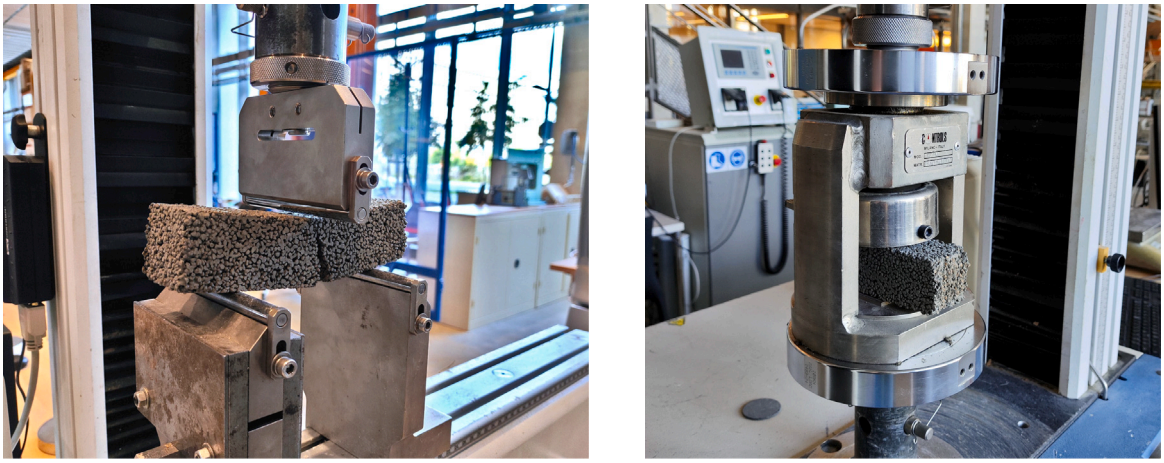

(a) (b)

Fig. 3. Setups employed to carry out flexural (a) and compressive (b) tests.

placed in an environment at 22 °C and 50% RH for 21 days, giving a total curing period of 28 days. Finally, the mass and volume of the samples were measured to derive the density of the hardened samples.

2.2.2. Ultrasonic pulse velocity test

Ultrasonic pulse velocity tests were carried out to derive the dynamic Young's modulus of mortar samples after 28 days of curing. The oscilloscope InfiniiVision DSO-X 2002A was used to generate pulses of longitudinal stress waves through the short side of the prismatic samples. Acoustic gel was preliminarily applied to the probes to facilitate the transmission of pulses. The pulse velocity V was calculated by dividing the distance L between the two probes by the transit time T. According to the standard ASTM 597-02 [41], Eq. (1) was used to derive the dynamic Young's modulus E_d:

$$E_d = \rho \cdot V^2 \cdot \frac{(1+\nu)\cdot(1-2\nu)}{1-\nu} \tag{1}$$

where ρ is the density of the hardened samples and ν is the Poisson's ratio.

2.2.3. Flexural and compressive tests

Mechanical tests were performed after 28 days of curing by means of a mechanical press equipped with the accessories shown in Fig. 3 on prismatic samples measuring 4 cm × 4 cm × 16 cm. Flexural tests were first conducted for all samples, and the resulting prism halves were used for the compression tests. The procedures were carried out according to UNI EN 1015-11:2019, considering a loading rate of 20 N/s and 200 N/s for flexural and compressive tests, respectively.

2.2.4. Thermal conductivity

Thermal conductivity was measured on both prismatic and cylindrical samples after 28 days of curing. Measurements were performed using the NeoTIM device, which relies on the hot wire method and whose working principle is derived from ASTM D5930-97 [42] and RILEM AAC 11-3 [43]. It adopts a hot wire probe capable of measuring thermal conductivity values ranging from 0.2 to 5 W/(m·K), for samples not smaller than 60 × 40 mm. Measurements were carried out on the basis of three prismatic and four cylindrical samples, utilizing various combinations of coupled faces to ensure that the most representative values of thermal conductivity were obtained.

(a) (b)

Fig. 4. Assessment of porosity through the hydrostatic weighing method: hydrostatic weighing (a), weighing in saturated surface-dried condition (b).

2.2.5. Porosity

The porosity of the composite OKA-based mortars was tested by means of the hydrostatic weighing method (water porosimetry), according to the French norm NF P18-459. Each of the cylindrical samples was positioned in a vacuum apparatus and degassed. Then, water at 22 °C was introduced while maintaining the reduced pressure. After 48 h of immersion, each sample was removed from the water bath and quickly placed in the basket (Fig. 4(a)) to measure its mass in water m_w. It was then taken out, gently wiped with a wet cloth, and placed on a scale to determine the saturated surface-dried mass m_{ssd} (Fig. 4(b)). All samples were then oven-dried at 60 °C until two successive weighings 24 h apart differed by less than 0.5%, and were finally weighed to obtain their oven-dried mass m_d.

The porosity ϕ was then derived according to Eq. (2).

$$\phi = \frac{m_{ssd} - m_d}{m_{ssd} - m_w} \tag{2}$$

2.2.6. Moisture buffer value and water vapor permeability

The determination of the Moisture Buffer Value (MBV) was carried out on cylindrical specimens according to the NORDTEST protocol [44]. This test consists of exposing one surface of the samples to cyclic humidity variations that replicate the daily cycles observed in buildings. Samples were first conditioned in a climatic chamber at 23 °C and 50% RH until two successive weight determinations at a 24 h interval differed by less than 0.1% of the mass of the specimen. Once stabilized, all the surfaces except one were sealed with aluminum tape as shown in Fig. 5(a). Then, the sealed samples were positioned in the climatic chamber at 23 °C and subjected to an ambient humidity of 33% RH for 16 h, followed by a period of 8 h at 75% RH, and their mass measured at the onset of each humidity change. This cycle was then repeated daily until three consecutive stable cycles, characterized by a daily mass variation of less than 5%, were observed. The practical value of the MBV was finally derived according to Eq. (3):

$$MBV = \frac{m_{max} - m_{min}}{A \cdot \Delta RH} \tag{3}$$

where m_{max} is the mass of the sample at the end of the 75% RH period, m_{min} is the mass of the sample at the beginning of the 75% RH period, and A is the area of the exposed surface.

The Water Vapor Permeability (WVP) was determined on cylindrical samples by means of the cup method, according to ISO 12572:2016 [45]. Before testing, samples were stored in a climatic chamber at 23 °C and 50% RH until three consecutive daily weight measurements agreed within 5%. Then, the lateral sides of samples were sealed with aluminum tape and positioned on top of cups containing an aqueous solution of ammonium dihydrogen phosphate ($NH_4H_2PO_4$), which allows to maintain a relative humidity of 94% at the bottom surface of the test specimen. Finally, the gaps between cups and cylindrical samples were sealed and the resulting test assemblies positioned in the climatic chamber at 23 °C and 50% RH. Then, the test procedure consisted of daily weighing until five successive mass determinations for each specimen were within ±5% of its mean value. The WVP was finally calculated on the basis of Eq. (4),

$$WVP = \frac{G \cdot d}{A \cdot \Delta p} \tag{4}$$

where G is the five-days moving average of the daily measured mass change rate, d is the sample thickness, A is the exposed area of the specimen and Δp is the water vapor pressure difference between the top and bottom surfaces of the sample, assumed equal to 1207 Pa in this test.

(a) (b)

Fig. 5. Measurement of MBV and water vapor resistance, respectively through the NORTDEST protocol (a) and the wet cup method (b).

2.2.7. SEM and morphological observations

Morphological observations were carried out by means of a scanning electron microscope (ZEISS EVO MA 10), equipped with a tungsten thermionic emission gun, focusing on the Interfacial Transition Zone (ITZ) between OKA particles and the cementitious matrix. Prior to analysis, the samples were embedded in epoxy resin and then polished using abrasive papers up to grit P2400. A final polishing step with diamond paste was performed to eliminate surface scratches. The samples were then mounted on aluminum stubs using silver conductive paint and coated with a thin layer of gold by cathodic sputtering to ensure good electrical conductivity. Images were captured at various magnifications (ranging from ×6.8 to ×1000) in secondary electron mode.

2.2.8. X-ray diffraction

A structural analysis was carried out by means of X-ray diffraction (XRD) using a Bruker D8 Advance diffractometer equipped with a Cu–Kα source ($\lambda = 1.5406$ Å), operating at 40 kV and 30 mA. Three types of samples were studied: (i) recovered cement matrix, (ii) recovered OKA particles, extracted from a F400A sample, and (iii) fresh OKA. Samples were prepared by gentle mechanical separation, followed by grinding (PM100, 600 rpm) and sieving at 63 μm, in accordance with standard NF EN 196-2.

The analysis was performed over an angular range from 10° to 80° (2θ), with an angular step of 0.02° and a counting time of 2 seconds per step. Each analysis was conducted on 50 mg of powder. This protocol allowed evaluation of the influence of the chemical composition of the OKA on the hydration process and the mineralogical evolution of the cementitious matrix.

3. Results

3.1. Hardened density

The hardened density values for all formulations are presented in Fig. 6(b), while a representative sample is shown in Fig. 6(a). Samples F500A showed the highest value of 1319 kg/m^3, while the lowest, 1060 kg/m^3, was observed for mortars F300B. Focusing on type A mortars (i.e., F500A, F400A, and F300A), it can be noted that the variation in density directly reflects the difference in binder dosage used for their production. Comparing type A and type B mortars, it is evident that for the same cement dosage, the density values of type B mortars are approximately 25 kg/m^3 lower than those of type A. This reduction is directly attributable to the lower bulk density of the fine OKA compared to the raw OKA, as shown in Table 1.

3.2. Porosity

Porosity values, measured as specified in Section 2.2.5, are well correlated with the hardened density, as shown in Fig. 7. The trend observed for type A mortars shows that porosity decreases with increasing cement dosage. Indeed, a value of 0.31 was observed for samples produced with 500 g of cement, increasing to 0.39 and 0.41 at a dosage of 400 g and 300 g, respectively. The comparison between the results obtained at cement dosages of 400 g and 300 g for mortars type A and B highlights an increase in porosity of about 2% when the fine OKA is employed.

3.3. Thermal conductivity

For type A samples, the thermal conductivity decreases proportionally to the amount of binder employed (Fig. 8), dropping from 0.411 W/(m·K) to 0.298 W/(m·K) at cement dosages of 500 g and 300 g, respectively. Measurements carried out on type B samples demonstrate that lower thermal conductivity values can be achieved if fine OKA is employed at a constant cement dosage. Indeed, sample F300B showed the lowest value of 0.28 W/(m·K).

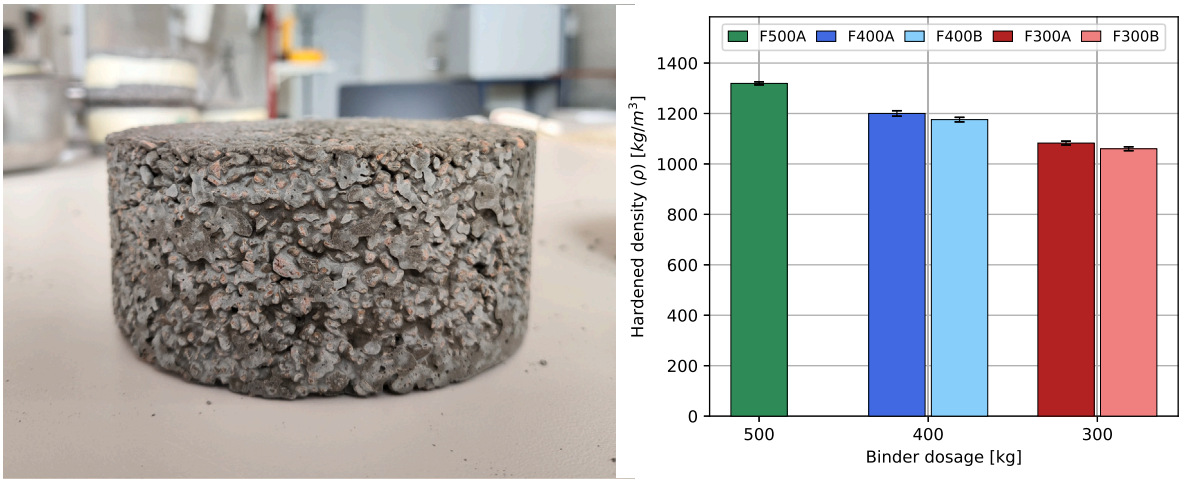

Fig. 6. Hardened olive kernel-based sample at the end of curing period (a), hardened density of the investigated formulations (b).

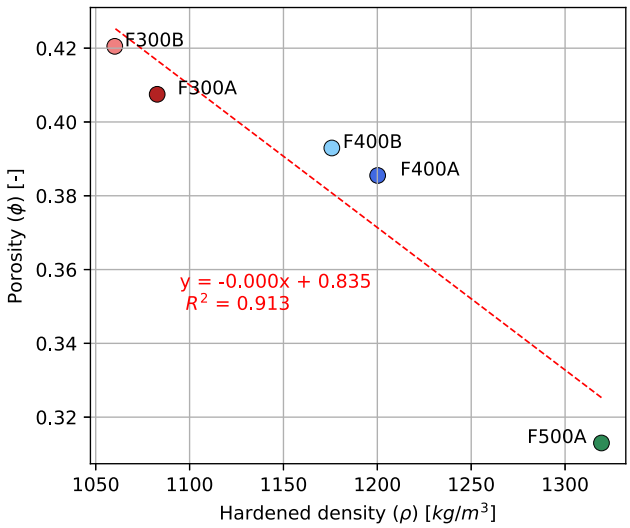

Fig. 7. Porosity of OKA-based mortars obtained by means of the hydrostatic weighing method.

3.4. Dynamic Young's modulus

The dynamic Young's modulus appears to be directly proportional to the binder dosage, as illustrated in Fig. 9, with the highest value of 6.80 GPa measured for samples F500A. Samples produced with fine OKA show lower E_d values compared to those produced with raw OKA at the same binder dosage. A decrease of about 14% was recorded at 400 g and 300 g binder dosages, and roughly 26% when 300 g of cement was used, with a minimum value of 1.89 GPa observed for samples F300B.

3.5. Flexural and compressive strength

Following the trend observed for the dynamic Young's modulus (Section 3.4), the mechanical performance of all tested samples is proportional to the dosage of binder employed, while the use of fine OKA has a negative impact compared to the results obtained for samples produced with raw OKA (see Fig. 10). Indeed, for type A mortars, the lowest performance was observed for sample F300A, which showed a flexural strength σ_f of 0.59 MPa and a compressive strength σ_c of 3.50 MPa. From this point, an increase of 100 g in the cement dosage led to a significant improvement in mechanical properties, with values of $\sigma_f = 1.85$ MPa and $\sigma_c = 13.69$ MPa measured for samples F400A. A further increase in mechanical properties was observed with higher cement dosage, which led to a flexural strength of $\sigma_f = 2.34$ MPa and a compressive strength of 19.15 MPa for samples F500A.

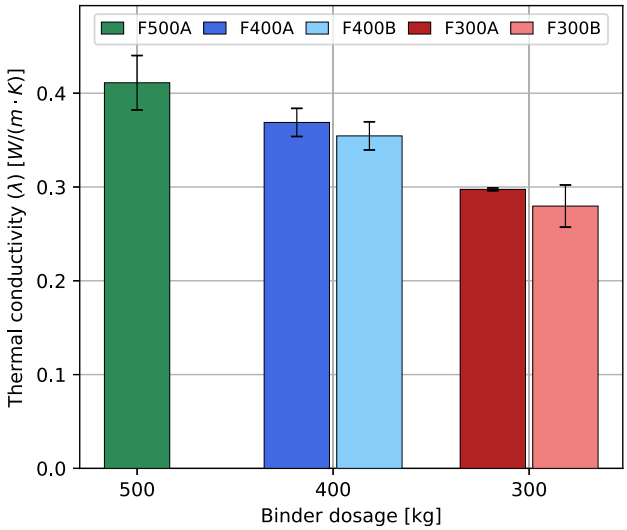

Fig. 8. Thermal conductivity of the hardened samples.

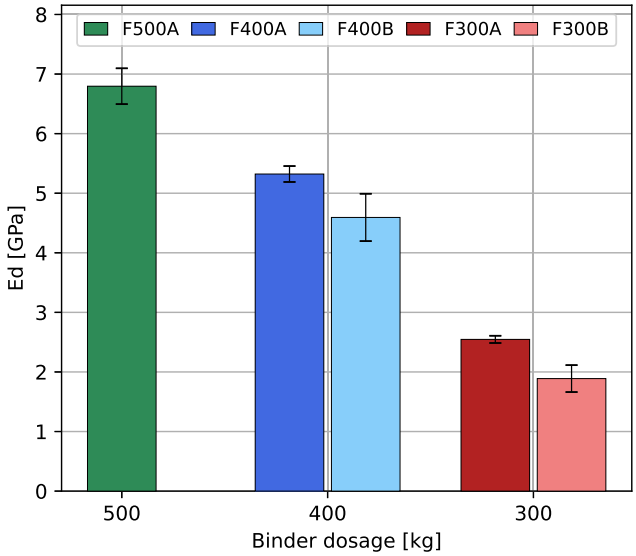

Fig. 9. Dynamic Young's modulus measured through the ultrasonic pulse velocity method.

The use of fine OKA reduced these values by about 12% and 26% at 400 g and 300 g binder dosages, respectively. The lowest mechanical properties were observed for samples F300B, with a flexural strength of 0.33 MPa and a compressive strength of 2.5 MPa.

3.6. MBV and WVP

Fig. 11 shows the MBV values of the OKA composites measured by means of the NORDTEST protocol. These are inversely proportional to the dosage of binder and show higher values if fine OKA is used at a constant cement dosage. The average value measured for samples F500A was 1.56, while the highest value, observed for samples F300B, was 2.88. According to the NORDTEST classification, composites F500A can be classified as good, while all other formulations possess excellent moisture buffer performance.

A similar trend can be observed for the WVP measured according to ISO 12572:2016, as shown in Fig. 12. Composites F500A show the lowest value of $0.75 \cdot 10^{-11}$ kg/(m·s·Pa), while the highest, equal to $1.7 \cdot 10^{-11}$ kg/(m·s·Pa), was obtained for mortars F300B. Moreover, at the same cement dosage, the substitution of raw OKA with its fine version leads to an increase in the WVP, especially when a cement dosage of 300 g is considered.

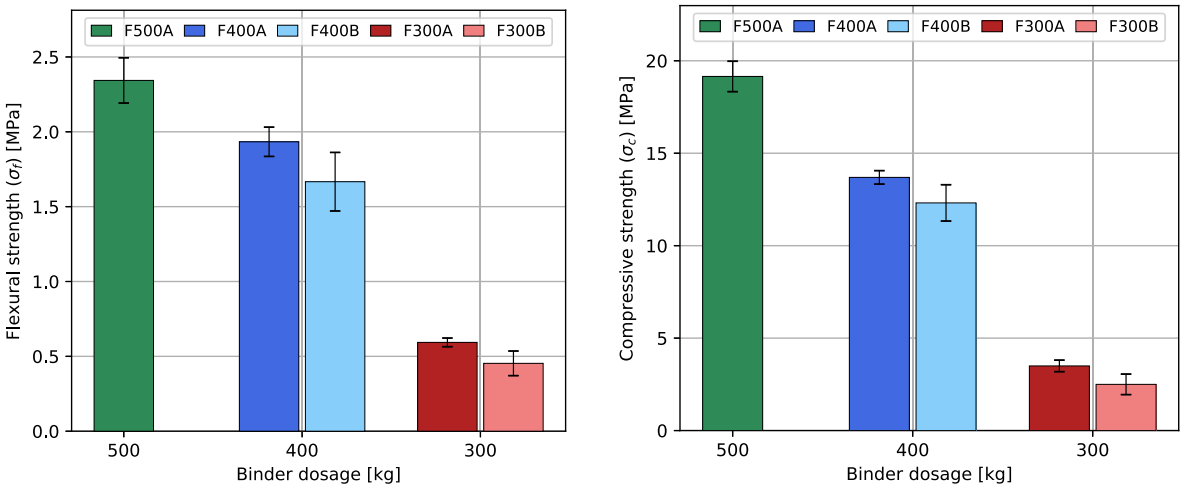

(a) (b)

Fig. 10. Flexural (a) and compressive (b) strength after 28 days of curing.

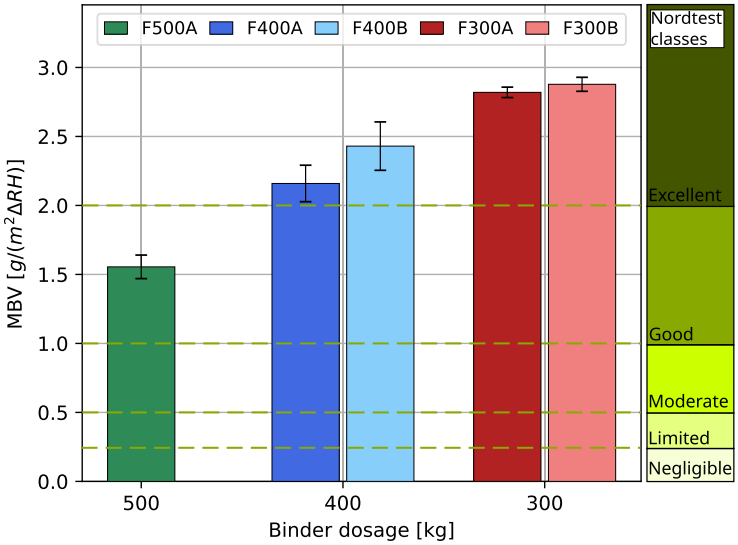

Fig. 11. Moisture Buffer Value of the tested samples and NORDTEST classification.

3.7. Morphological analysis

SEM observations were conducted on fractured cross-sections of F400A mortar samples to investigate the microstructure of the composite and the interfacial bonding between OKA particles and the cementitious matrix. Fig. 13(a), obtained at a magnification of ×6.8, gives an overall view of the phases of the composite, consisting of OKA particles, cement matrix, and voids. Moreover, debonding at the ITZ is visible at this stage. Figs. 13(b) and 13(c), acquired respectively at a magnification of ×17 and ×150, highlight pores and cracks in the cementitious matrix. Finally, at a magnification of ×1000, Fig. 13(d) clearly shows the low quality of the ITZ and the porous nature of the OKA particles.

3.8. XRD structural analysis

The XRD analysis of the OKA, presented in Fig. 14, reveals characteristic peaks at $2\theta = 14.5°$, 16.5° and 22.5°, corresponding to cellulose Iβ. The relative intensity of cellulose peaks decreases by approximately 20% for recovered OKA compared with fresh OKA, suggesting slight degradation during cement hydration.

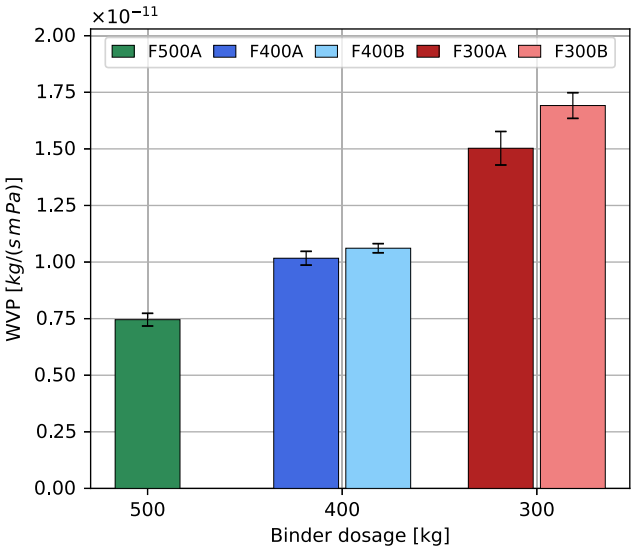

Fig. 12. Water vapor permeability of the OKA-based mortars samples.

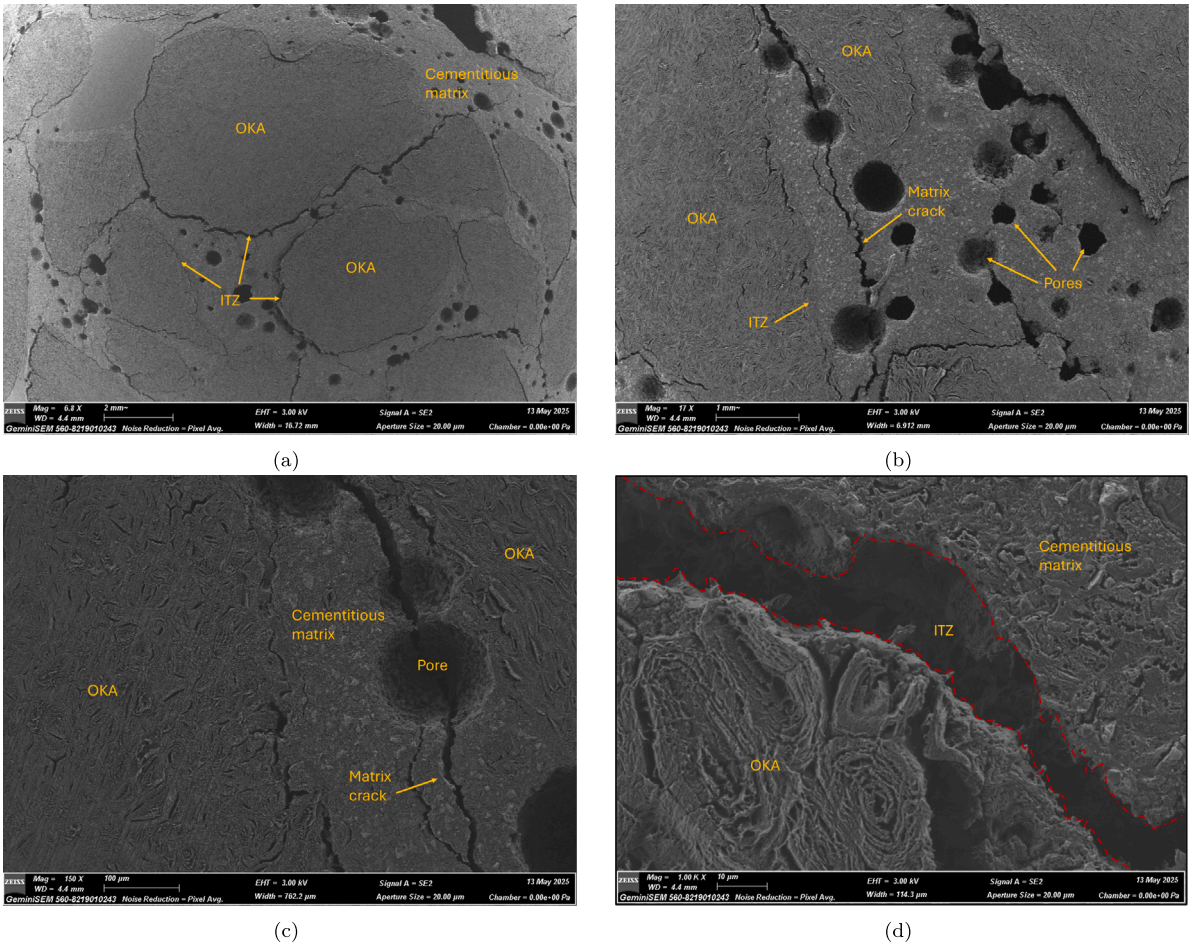

Fig. 13. SEM images of sample F400A, captured with magnifications of: ×6.8 (a), ×17 (b), ×150 (c) and ×1000 (d).

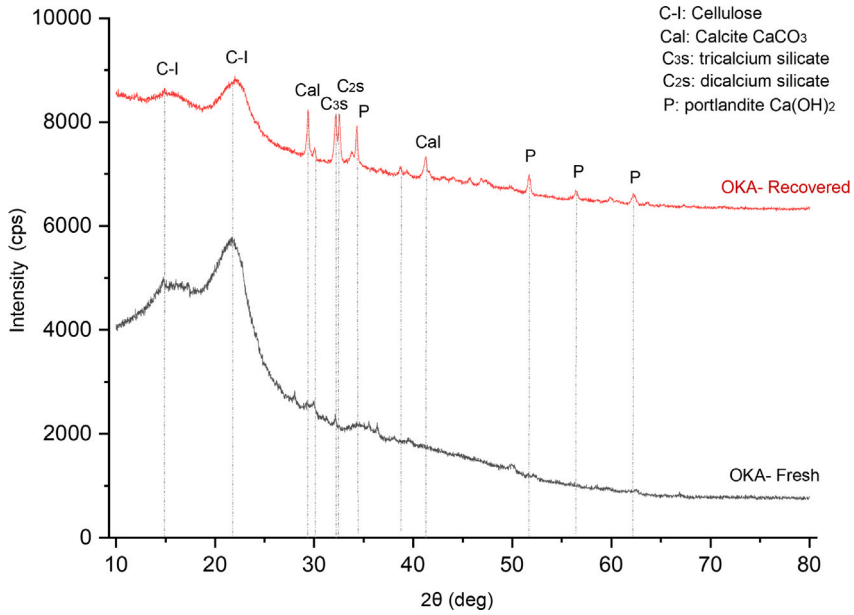

Fig. 14. XRD diffractogram of fresh and recovered OKA particles.

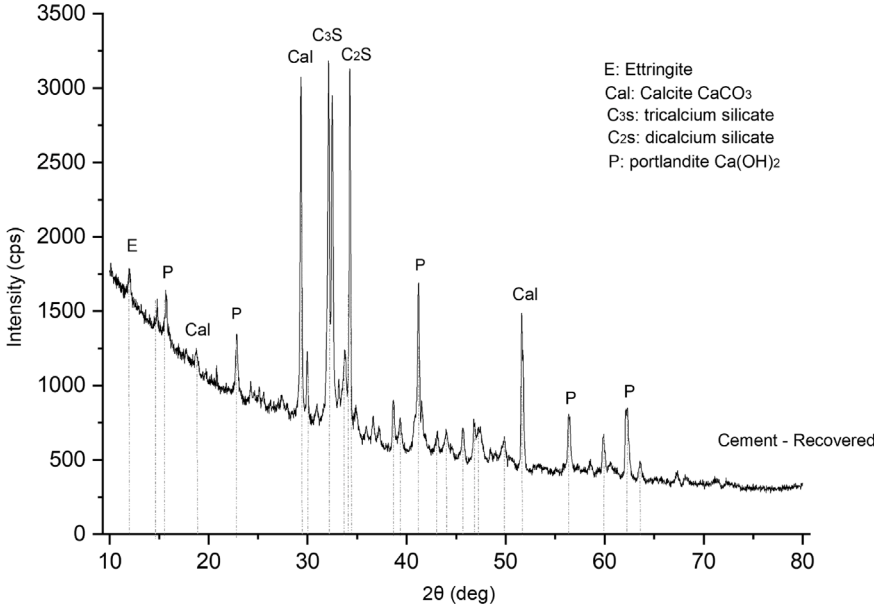

Fig. 15. XRD diffractogram of recovered cement matrix.

The cement matrix analysis in Fig. 15 shows characteristic phases of hydrated Portland cement: intense peaks at 18.1° and 34.1° attributed to portlandite ($Ca(OH)_2$), an amorphous halo centered at 29° characteristic of C–S–H gels, and residual ettringite peaks at 9.1° and 15.8°. The absence of new crystalline peaks and the stability of lattice parameters (shift less than 0.1° in 2θ) demonstrates no significant chemical interaction between OKA organic compounds and cement mineral phases. The full width at half maximum (FWHM) of peaks remains unchanged, confirming preserved crystallinity. These observations are consistent with previous studies on cement–biomass composites.

4. Discussion

As discussed in Section 3.1, the density of hardened samples is proportional to the binder content and decreases if fine OKA is employed due to its lower bulk density; the highest value of 1319 kg/m^3 was registered for mortars F500A. This value, taking into

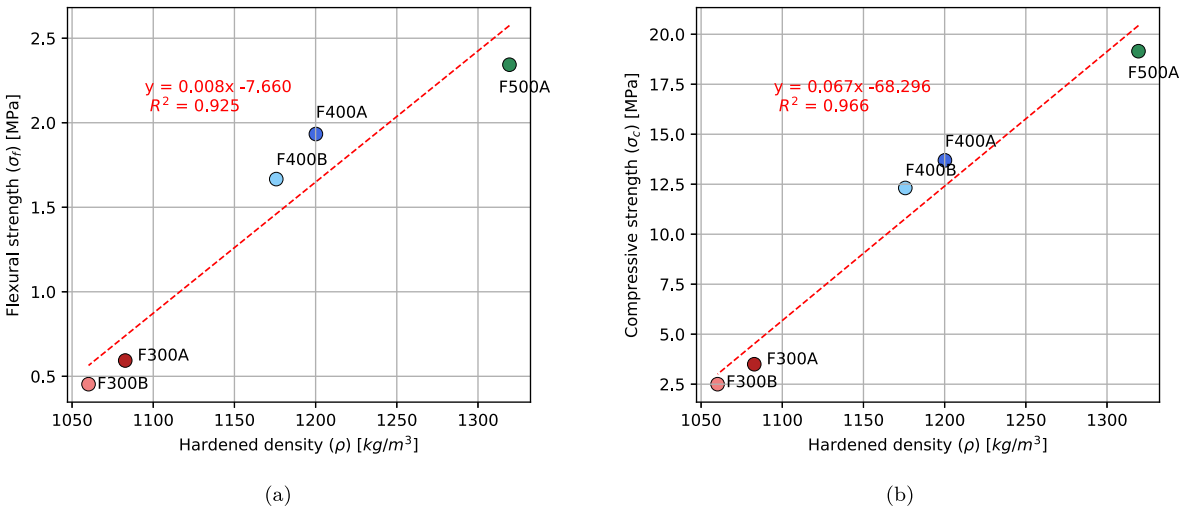

Fig. 16. Hardened density correlated with flexural (a) and compressive (b) strength.

account the influence of the cement dosage, is in line with that obtained for the 100% OKA-based mortars with an approximate cement dosage of 650 kg/m^3 studied by Cheboub et al. [33], for which the authors reported a density of 1410 kg/m^3. However, it must be considered that Cheboub et al. reported the dry density, whereas in this work samples were weighed at the end of the 28-day curing period without oven drying. In other research where sand was partially replaced (30% substitution) with 330 kg/m^3 of cement, the density was about 1790 kg/m^3 [31], while in [32], with a dosage of 678 kg/m^3 of cement and 50% OKA replacement, the hardened density was 1500 kg/m^3.

Mechanical properties appear to be closely correlated with the hardened density, as shown in Fig. 16. This trend might be interpreted as follows: the density increases with cement dosage, as shown in Section 3.1, and at increasing cement dosages the W/C ratio is reduced to maintain the same workability (see Table 2), promoting higher mechanical performance. Moreover, mortars were not conceived as standard concrete, for which solid constituents are proportioned to achieve maximum compaction. Instead, in this work, the reduction of the cement dosage was the main objective in the mix design, which led to mortars characterized by high porosity (see Fig. 7). In this scenario, alongside the effect of the W/C ratio, the filling action of cement might have a considerable influence on the resulting mechanical performance. In addition to this, the interaction between OKA particles and the cementitious matrix plays a crucial role in the macroscopic mechanical properties. While in Section 3.8 it was assessed that cement hydration is not affected by the organic nature of the OKA, SEM observations in Section 3.7 revealed cracks in the matrix, as well as a low-quality ITZ. These defects might be due to the hydrophilic nature of the aggregate, possibly worsened by dimensional variations associated with changes in water content in the composite. It is therefore reasonable to assume that actions taken to improve the quality of the ITZ could lead to enhanced mechanical properties.

Nevertheless, the results are encouraging. The mortars investigated in this work achieved up to 19.15 MPa in compression with a cement dosage of 500 kg/m^3. This is particularly significant when comparing the results in Fig. 16 with comparable studies. Indeed, Ferreiro-Cabello et al. [31], using the same cement type (CEM I 52.5 R) but with only 30% substitution of natural sand, reported a compressive strength of 12 MPa and flexural strength of 1.4 MPa at 28 days, with approximately 330 kg/m^3 of cement.

In [32], authors used about 678 kg/m^3 of CEM II/A 42.5 cement and gradually substituted sand with OKA. At 50% substitution, they obtained a compressive strength of 15 MPa. The most relevant comparison is with Cheboub et al. [33], the only other study achieving complete substitution of sand with OKA. Based on their data, a cement dosage exceeding 650 kg/m^3 (CEM II/B 42.5 N) can be estimated. At 100% OKA substitution, they achieved a compressive strength of 7 MPa and a flexural strength of 3 MPa at 28 days (increasing to 15 MPa at 91 days). In the present work, as shown in Fig. 16, the same compressive strength at 28 days could be achieved with a cement dosage of only about 350 kg/m^3.

Furthermore, regarding sustainability, the clinker content of the CEM II/A cement employed in [33] ranges between 65% and 79% according to EN 197-1. Consequently, their estimated clinker content lies between 420 and 513 kg/m^3. Conversely, for the mortars in this work using CEM I (approx. 95% clinker), the same compressive strength at 28 days would be achieved with a clinker content of about 332 kg/m^3. Since clinker is the primary source of CO_2 emissions, this demonstrates the improved sustainability of the proposed formulations compared to previous studies, despite the use of Portland cement. Future research could further reduce the carbon footprint by exploring more sustainable binders.

Overall, the results suggest that mortars produced with a cement dosage above 350 kg/m^3 may be suitable for moderate load-bearing applications in buildings, such as lightweight floor screeds. The European standard EN 13813:2002 sets minimum flexural and compressive strengths for screeds at 1 MPa and 5 MPa, respectively. In this context, mortars produced with 400 kg/m^3 of cement achieved a compressive strength at 28 days of approximately 13 MPa, well above the minimum requirements. For comparison,

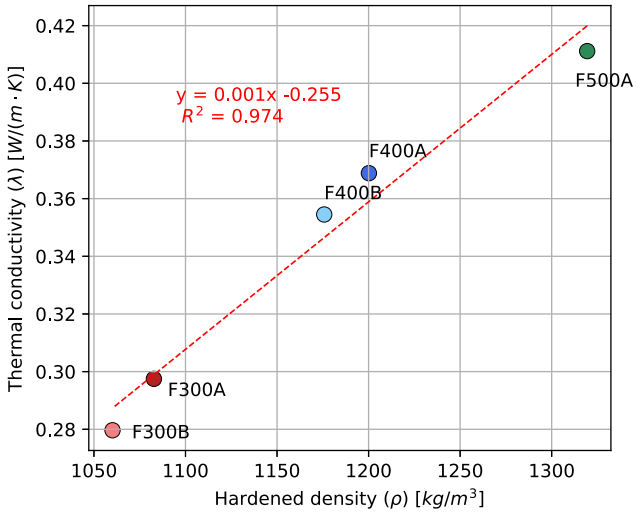

Fig. 17. Correlation between hardened density and thermal conductivity.

the 100% OKA-based mortars reported in [33] reached about 7 MPa at 28 days but required a significantly higher binder dosage (≈650 kg/m^3).

The thermal conductivity of the hardened samples is proportional to the hardened density, as shown in Fig. 17. This is in line with results obtained in [46] for hemp shive composites, in [47] for walnut shell mortars, and in [30,32,33] for OKA-based mortars. Specifically, OKA-based mortars in [30] (70% sand substitution) showed a thermal conductivity of 0.266 W/(m·K) at 1148 kg/m^3. In [32] (50% substitution), the conductivity was 0.689 W/(m·K) at 1500 kg/m^3, while in [33] (100% substitution), it was 0.35 W/(m·K) at 1410 kg/m^3. These values align with the thermal conductivity measured in this work, ranging from 0.28 to 0.41 W/(m·K) at 1060 and 1319 kg/m^3, respectively. Overall, this represents a significant improvement in thermal insulation compared to traditional sand-based cementitious mortars, which typically exhibit values between 1.5 and 2 W/(m·K).

Regarding hygric properties, although results in Section 3.6 are presented in terms of Water Vapor Permeability (WVP), the discussion relies on the water vapor resistance factor (μ) to allow for a direct comparison with literature data. The μ-value is calculated as the ratio of the water vapor permeability of air ($\delta_a \approx 1.95 \cdot 10^{-10}$ kg/(m·s·Pa)) to the WVP of the material ($\mu = \delta_a / WVP$). The lowest μ-value (11.66) was observed for the lightest formulation (F300B), while the highest (26.47) was registered for F500A. Comparison with common building materials highlights the behavior of these composites: according to [48,49], the μ-value is about 150 for XPS, 50 for EPS, 100 for polyurethane, 10 for thermal insulating plaster, and 45–88 for standard cementitious mortars. Bio-based materials typically show lower values, e.g., 3.8–4.4 for hemp concrete [50] or 8–9 for straw-lime concrete [51]. The mortars in this study thus possess a permeability much higher than expanded polymeric panels and standard mortars, though not as high as ultra-lightweight bio-based composites.

As noted in Fig. 18, WVP values are well correlated with the Moisture Buffer Value (MBV). The mortars studied here possess good to excellent moisture buffering capabilities. While concrete typically has an MBV of 0.38 and gypsum 0.64 [44], the minimum value in this research was 1.56 (F500A) and the highest was 2.88 (F300B). According to the NORDTEST classification [44], formulation F500A is classified as *Good*, while all other formulations are *Excellent*. Combined with good vapor permeability and thermal properties, these materials can play an important role in controlling indoor humidity and improving energy efficiency. These combined hygrothermal properties suggest that OKA-based mortars produced with reduced cement dosages are suitable for lightweight insulating panels or direct application onto building envelopes, combining moisture regulation with thermal performance.

Overall, the results indicate that lower cement dosages optimize hygrothermal properties, while higher dosages enhance mechanical strength, suggesting distinct potential applications in buildings. (i) Formulations F300A and F300B (or lighter variants) could replace cellular concrete as lightweight filling screeds or in roof build-ups (plane or sloped). Their stiff consistency in the fresh state facilitates application on slopes, and their thermal inertia, expected to be higher than that of EPS or rockwool, would improve envelope performance in warm seasons. Application as vertical plaster is currently not suggested due to rheological constraints. (ii) Conversely, cement dosages above 350 kg/m^3 are suitable for moderate load-bearing applications. An OKA-based mortar with ≈350 kg/m^3 cement would likely meet EN 13813 requirements for compressive class C5 and flexural class F1, while formulation F500A would fall into classes C16/F2. Intermediate dosages could be employed for masonry units to construct lightweight walls with improved thermal insulation and humidity control.

A summary of the results obtained in this work is presented in Fig. 19 by means of a correlation matrix, where the dependence of each property or parameter on the others is summarized by the respective correlation coefficient. For the reader's convenience, the notation used throughout the paper is recalled as follows: ρ denotes the hardened density of samples, CEM the cement dosage, σ_f the flexural strength, σ_c the compressive strength, E_d the dynamic Young's modulus, λ the thermal conductivity, WVP the water vapor permeability, MBV the moisture buffer value, ϕ the porosity of the hardened samples and W/C the water/cement ratio.

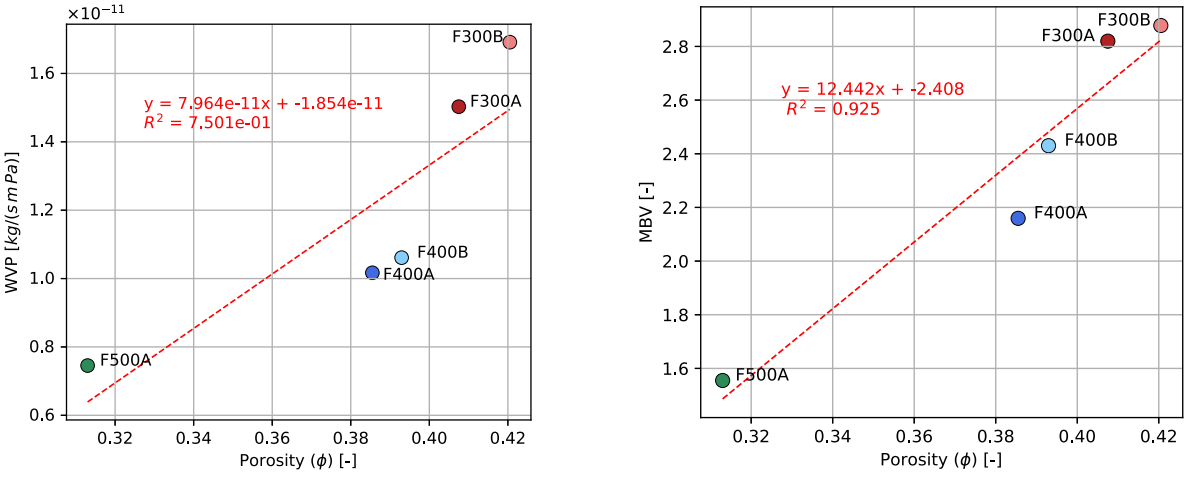

Fig. 18. Influence of porosity on water vapor permeability (a) and moisture buffer value (b).

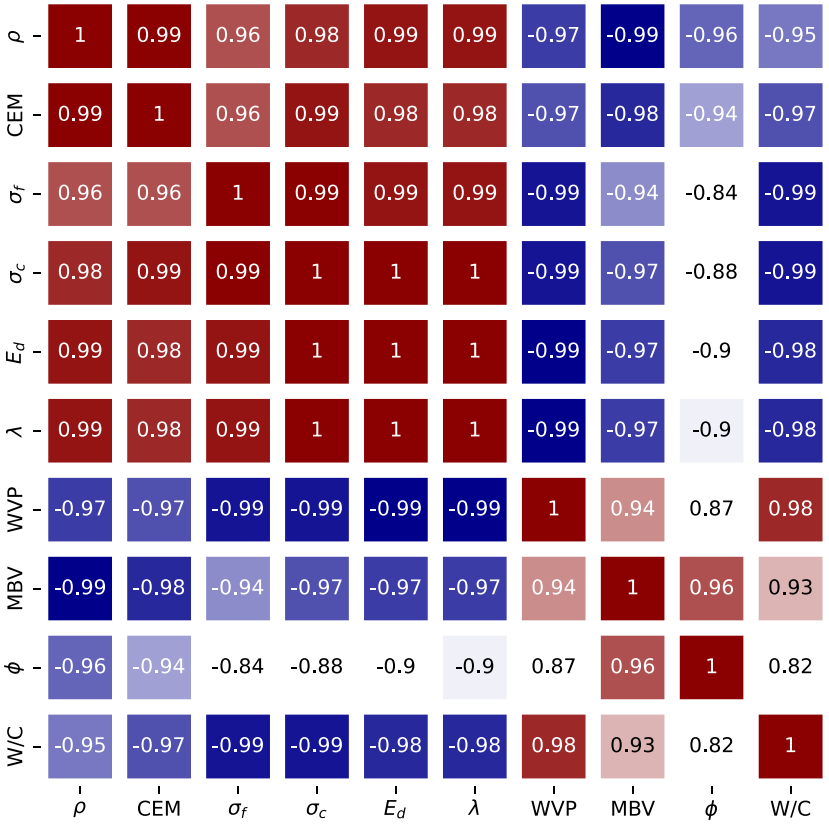

Fig. 19. Correlation matrix of properties and parameters of OKA-based composites studied in this research.

5. Conclusions

An extensive experimental campaign was carried out on cementitious mortars employing a by-product of olive oil manufacturing as aggregate, namely Olive Kernel Aggregate (OKA). The study investigated the influence of both cement dosage and granulometric distribution of OKA on the resulting material performance. Mechanical and hygrothermal properties were determined, complemented

by SEM observations of the composite microstructure and XRD analyses to assess binder–aggregate compatibility. The results demonstrate that excellent mechanical performance can be achieved even with cement dosages considerably lower than those adopted in the few references available in the literature on OKA-based mortars. In particular, In particular, the clinker content of formulation F400A is significantly lower than that estimated for the 100% OKA-based mortar studied by Cheboub et al. [33] (the only work reporting a complete substitution of sand), while achieving higher compressive strength at 28 days. Considering that clinker is the main contributor to the carbon footprint of cement, this result highlights the improved sustainability of the formulations investigated in this research. From a hygrothermal perspective, the mortars exhibit high water vapor permeability and excellent moisture buffering capacity. Notably, the Moisture Buffer Value (MBV), which had never previously been assessed for this type of mortar, reached values classified as *Excellent* according to the NORDTEST protocol. The combined mechanical and hygrothermal characterization shows that, by varying the cement dosage, it is possible to tailor the material either toward enhanced insulation and moisture-regulating properties or toward improved mechanical strength. This versatility allows different potential applications in buildings, ranging from lightweight insulating materials to moderate load-bearing components such as insulating screeds. Cement was employed in this research to enable direct comparison with previous studies and because of its wide availability and ease of use on construction sites. Nevertheless, future developments could focus on OKA-based mortars produced with more sustainable binders, such as alkali-activated binders. Although these systems are currently less widespread and require handling alkaline activating solutions rather than water, they may further reduce the environmental impact of these composites. Further research should also address long-term durability and dimensional stability under environmental conditions, in order to confirm the effective suitability of OKA-based mortars for practical building applications.

CRediT authorship contribution statement

Nicolò Lo Presti: Writing – review & editing, Writing – original draft, Visualization, Methodology, Investigation, Formal analysis, Conceptualization. **Kamilia Abahri:** Writing – review & editing, Writing – original draft, Supervision, Resources, Methodology, Formal analysis. **Mohamed Soufiane Ghomchi:** Writing – review & editing, Visualization, Investigation. **Paolo Stabellini:** Writing – review & editing, Resources, Funding acquisition. **Giovanni Castellazzi:** Writing – review & editing, Writing – original draft, Supervision, Methodology, Funding acquisition.

Declaration of competing interest

The authors declare that they have no known competing financial interests or personal relationships that could have appeared to influence the work reported in this paper.

Acknowledgments

Funded by the European Union - Next Generation EU, Mission 4, Component 2, Investment 3.3 (Ministerial Decree 117/2003) CUP J33C22001430009. This work was also funded by EDILTECO S.p.A. The authors gratefully acknowledge Marc Bonnet and Thomas Reiss for their valuable assistance with SEM and XRD.

Data availability

Data will be made available on request.

References

[1] A. Dyson, N. Keena, M.-l. Lokko, B. K. Reck, C. Ciardullo, Building Materials and the Climate: Constructing a New Future, Tech. Rep., Yale CEA, 2023.
[2] P. Peduzzi, Sand, rarer than one thinks, Environ. Dev. 11 (208–218) (2014) 682.
[3] M.D. Gavriletea, Environmental impacts of sand exploitation. Analysis of sand market, Sustainability 9 (7) (2017) 1118.
[4] S.A. Ishak, H. Hashim, Low carbon measures for cement plant–a review, J. Clean. Prod. 103 (2015) 260–274.
[5] R. Snellings, P. Suraneni, J. Skibsted, Future and emerging supplementary cementitious materials, Cem. Concr. Res. 171 (2023) 107199.
[6] K. Scrivener, F. Martirena, S. Bishnoi, S. Maity, Calcined clay limestone cements (LC3), Cem. Concr. Res. 114 (2018) 49–56.
[7] A. Mohammadi, A.M. Ramezanianpour, Investigating the environmental and economic impacts of using supplementary cementitious materials (SCMs) using the life cycle approach, J. Build. Eng. 79 (2023) 107934.
[8] K. McNeil, T.H.-K. Kang, Recycled concrete aggregates: A review, Int. J. Concr. Struct. Mater. 7 (2013) 61–69.
[9] K.P. Verian, W. Ashraf, Y. Cao, Properties of recycled concrete aggregate and their influence in new concrete production, Resour. Conserv. Recycl. 133 (2018) 30–49.
[10] G. Churkina, A. Organschi, C.P. Reyer, A. Ruff, K. Vinke, Z. Liu, B.K. Reck, T. Graedel, H.J. Schellnhuber, Buildings as a global carbon sink, Nat. Sustain. 3 (4) (2020) 269–276.
[11] J.H. Arehart, J. Hart, F. Pomponi, B. D'Amico, Carbon sequestration and storage in the built environment, Sustain. Prod. Consum. 27 (2021) 1047–1063.
[12] S. Amziane, M. Sonebi, Overview on biobased building material made with plant aggregate, RILEM Tech. Lett. 1 (2016) 31–38.
[13] S. Bourbia, H. Kazeoui, R. Belarbi, A review on recent research on bio-based building materials and their applications, Mater. Renew. Sustain. Energy 12 (2) (2023) 117–139.
[14] A. Rima, K. Abahri, F. Bennai, C. El Hachem, M. Bonnet, Microscopic estimation of swelling and shrinkage of hemp concrete in response to relative humidity variations, J. Build. Eng. 43 (2021) 102929.

[15] S.R. Latapie, V. Sabathier, A. Abou-Chakra, Bio-based building materials: A prediction of insulating properties for a wide range of agricultural by-products, J. Build. Eng. 86 (2024) 108867.
[16] M.P. Tinoco, T.C. Cavalcante, L.D. de Andrade, O.M. de Araújo, R.T. Lopes, R.D. Toledo Filho, O.A.M. Reales, Mix design strategies for 3D printable bio-based cementitious composites using rice husk particles as multifunctional aggregates, J. Build. Eng. 100 (2025) 111740.
[17] F. Benmahiddine, F. Bennai, R. Cherif, R. Belarbi, A. Tahakourt, K. Abahri, Experimental investigation on the influence of immersion/drying cycles on the hygrothermal and mechanical properties of hemp concrete, J. Build. Eng. 32 (2020) 101758.
[18] Z. Alshndah, F. Becquart, N. Belayachi, Recycling of wheat straw aggregates of end-of-life vegetal concrete: Experimental investigation to develop a new building insulation material, J. Build. Eng. 76 (2023) 107199.
[19] K. Lila, S. Belaadi, R. Solimando, F.R. Zirour, Valorisation of organic waste: Use of olive kernels and pomace for cement manufacture, J. Clean. Prod. 277 (2020) 123703.
[20] E. Farag, M. Alshebani, W. Elhrari, A. Klash, A. Shebani, Production of particleboard using olive stone waste for interior design, J. Build. Eng. 29 (2020) 101119.
[21] A. San Vicente-Navarro, M. Mendívil-Giro, J. Los Santos-Ortega, E. Fraile-García, J. Ferreiro-Cabello, Alternative use of the waste from ground olive stones in doping mortar bricks for sustainable Façades, Buildings 13 (12) (2023) 2992.
[22] A. San Vicente-Navarro, J. Los Santos-Ortega, E. Fraile-García, J. Ferreiro-Cabello, Methodology for sustainability assessment for the use of ground olive stones in mortar bricks for facades, Appl. Sci. 14 (8) (2024) 3388.
[23] H. Al-Mattarneh, M. Abuaddous, R. Ismail, A.B. Malkawi, Y. Jaradat, H. Nimer, M. Khodier, Performance of concrete paving materials incorporating biomass olive oil waste ash and nano-silica, AIMS Mater. Sci. 11 (5) (2024).
[24] F. Safouene, S. Saedi, Investigating olive waste ash as a sustainable additive in rigid pavement design, Met. Mater. Eng. 30 (4) (2024) 553–565.
[25] A.M. Mohamed, B.A. Tayeh, Y.I.A. Aisheh, M.N.A. Salih, Utilising olive-stone biomass ash and examining its effect on green concrete: A review paper, J. Mater. Res. Technol. 24 (2023) 7091–7107.
[26] M. El Fessikh, H. Elhrech, A.E.Y. El Idrissi, L.-H. Lee, W. Al Abdulmonem, N. El Omari, A. Bouyahya, Sustainable valorization of olive stone by-products: Opportunities and challenges, J. Food Comp. Anal. 142 (2025) 107495.
[27] J. Los Santos-Ortega, E. Fraile-García, J. Ferreiro-Cabello, Environmental assessment of the use of ground olive stones in mortars. Reduction of CO2 emissions and production of sustainable mortars for buildings, Environ. Impact Assess. Rev. 110 (2025) 107709.
[28] M. Martin-Morales, G.M. Cuenca-Moyano, M.J. Martinez-Echevarria, M. Zamorano, M. Lopez-Alonso, Valorization of olive stone in cement mortars for harmonized applications, Materials 18 (22) (2025) 5200.
[29] M. del Río Merino, J.G. Rodríguez, F.F. Martínez, J.S.C. Astorqui, Viability of using olive stones as lightweight aggregate in construction mortars, Rev. de la Constr. 16 (3) (2017) 431–438.
[30] F. Barreca, C. Fichera, Use of olive stone as an additive in cement lime mortar to improve thermal insulation, Energy Build. 62 (2013) 507–513.
[31] J. Ferreiro-Cabello, E. Fraile-Garcia, F.J. Martinez-de Pison, et al., Strength performance of different mortars doped using olive stones as lightweight aggregate, Buildings 12 (10) (2022) 1668.
[32] D. Boukhelkhal, M. Guendouz, A. Bourdot, H. Cheriet, K. Messaoudi, Elaboration of bio-based building materials made from recycled olive core, MRS Energy & Sustain. 8 (2021) 98–109.
[33] T. Cheboub, Y. Senhadji, H. Khelafi, G. Escadeillas, Investigation of the engineering properties of environmentally-friendly self-compacting lightweight mortar containing olive kernel shells as aggregate, J. Clean. Prod. 249 (2020) 119406.
[34] N. Lo Presti, K. Abahri, G. Castellazzi, P. Mengoli, P. Stabellini, Experimental investigation of lightweight mortars based on recycled olive kernel through hygric and mechanical characterization, Adv. Sci. Technol. 159 (2025) 27–32.
[35] ISO 20290-1:2021 - UNI Ente Italiano di Normazione. URL https://store.uni.com/iso-20290-1-2021.
[36] UNI EN 1097-6:2022 - UNI Ente Italiano di Normazione. URL https://store.uni.com/uni-en-1097-6-2022.
[37] Y. Jiang, M. Lawrence, A. Hussain, M. Ansell, P. Walker, Comparative moisture and heat sorption properties of fibre and shiv derived from hemp and flax, Cellulose 26 (2) (2019) 823–843.
[38] W. Zillig, Moisture Transport in Wood Using a Multiscale Approach, Building Physics; Katholieke Universiteit Leuven, Leuven, Belgium, 2009.
[39] UNI EN 196-1:2016 - UNI Ente Italiano di Normazione. URL https://store.uni.com/uni-en-196-1-2016.
[40] UNI EN 1015-11:2019 - UNI Ente Italiano di Normazione. URL https://store.uni.com/uni-en-1015-11-2019.
[41] C597 standard test method for pulse velocity through concrete. URL https://www.astm.org/c0597-16.html.
[42] D5930 standard test method for thermal conductivity of plastics by means of a transient line-source technique. URL https://www.astm.org/d5930-97.html.
[43] Rilem, AAC 11.3 Determination of the thermal conductivity of oven dry AAC (dynamic method), in: RILEM Technical Recommendations for the Testing and Use of Construction Materials, CRC Press, 2020, http://dx.doi.org/10.1201/9781482271362-105/AAC-11-3-DETERMINATION-THERMAL-CONDUCTIVITY-OVEN-DRY-AAC-DYNAMIC-METHOD-RILEM, 440–440.
[44] C. Rode, R. Peuhkuri, H. Lone, B. Time, A. Gustavsen, T. Ojanen, J. Ahonen, K. Svennberg, L.-E. Harderup, J. Arfvidsson, Moisture Buffering of Building Materials, Technical University of Denmark DTU, 2006.
[45] UNI EN ISO 12572:2016 - UNI Ente Italiano di Normazione. URL https://store.uni.com/uni-en-iso-12572-2016.
[46] M. Kubiś, P. Łapka, Ł. Cieślikiewicz, G. Sahmenko, M. Sinka, D. Bajare, Analysis of the thermal conductivity of a bio-based composite made of hemp shives and a magnesium binder, Energies 15 (15) (2022) 5490.
[47] M.Y. Abdulwahid, S.F. Abdullah, The utilization of walnut shells as a partial replacement of sand in mortar mixes, Struct. Concr. 22 (2021) E300–E307.
[48] ANIT - Associazione Nazionale per l'Isolamento Termico e acustico, Parte 7: Schede dei materiali, 2015, https://www.anit.it/wp-content/uploads/2015/02/Parte-7_v3.pdf. (Accessed 2 February 2026).
[49] N. Issaadi, A. Nouviaire, R. Belarbi, A. Aït-Mokhtar, Moisture characterization of cementitious material properties: Assessment of water vapor sorption isotherm and permeability variation with ages, Constr. Build. Mater. 83 (2015) 237–247.
[50] A. Ruus, T. Koosapoeg, M. Pau, T. Kalamees, M. P ldaru, Influence of production on hemp concrete hygrothermal properties: sorption, water vapour permeability and water absorption, J. Phys.: Conf. Ser. 2069 (1) (2021) 012004.
[51] D. Jiang, P. An, S. Cui, S. Sun, J. Zhang, T. Tuo, Effect of modification methods of wheat straw fibers on water absorbency and mechanical properties of wheat straw fiber cement-based composites, Adv. Mater. Sci. Eng. 2020 (1) (2020) 5031025.